



## Environmental turbulent mixing controls on air-water gas exchange in marine and aquatic systems

Christopher J. Zappa,<sup>1</sup> Wade R. McGillis,<sup>1</sup> Peter A. Raymond,<sup>2</sup> James B. Edson,<sup>3</sup> Eric J. Hints,<sup>4</sup> Hendrik J. Zemmelenk,<sup>5,6</sup> John W. H. Dacey,<sup>7</sup> and David T. Ho<sup>1</sup>

Received 1 December 2006; revised 5 February 2007; accepted 5 April 2007; published 17 May 2007.

[1] Air-water gas transfer influences CO<sub>2</sub> and other climatically important trace gas fluxes on regional and global scales, yet the magnitude of the transfer is not well known. Widely used models of gas exchange rates are based on empirical relationships linked to wind speed, even though physical processes other than wind are known to play important roles. Here the first field investigations are described supporting a new mechanistic model based on surface water turbulence that predicts gas exchange for a range of aquatic and marine processes. Findings indicate that the gas transfer rate varies linearly with the turbulent dissipation rate to the <sup>1</sup>/<sub>4</sub> power in a range of systems with different types of forcing - in the coastal ocean, in a macro-tidal river estuary, in a large tidal freshwater river, and in a model (i.e., artificial) ocean. These results have important implications for understanding carbon cycling.

**Citation:** Zappa, C. J., W. R. McGillis, P. A. Raymond, J. B. Edson, E. J. Hints, H. J. Zemmelenk, J. W. H. Dacey, and D. T. Ho (2007), Environmental turbulent mixing controls on air-water gas exchange in marine and aquatic systems, *Geophys. Res. Lett.*, 34, L10601, doi:10.1029/2006GL028790.

### 1. Introduction

[2] The importance of global CO<sub>2</sub> uptake by the ocean is well-established in the literature, yet significant uncertainty remains in predicting its magnitude [Feely *et al.*, 2001; Ho *et al.*, 2006; Sweeney *et al.*, 2007; Takahashi *et al.*, 2002]. Recent research has also highlighted the importance of riverine CO<sub>2</sub> evasion to regional and global carbon budgets [Borges *et al.*, 2005; Cole and Caraco, 2001; Frankignoulle *et al.*, 1998; Richey *et al.*, 2002], with current estimates being comparable to the global oceanic CO<sub>2</sub> sink. However, the accuracy of these studies is generally limited by their ability to adequately resolve the rate of gas transfer and the variability in aqueous CO<sub>2</sub> [Raymond and Cole, 2001; Richey *et al.*, 2002].

<sup>1</sup>Lamont-Doherty Earth Observatory, Columbia University, Palisades, New York, USA.

<sup>2</sup>School of Forestry and Environmental Studies, Yale University, New Haven, Connecticut, USA.

<sup>3</sup>Department of Marine Sciences, University of Connecticut, Groton, Connecticut, USA.

<sup>4</sup>Department of Chemistry and Chemical Biology, Harvard University, Cambridge, Massachusetts, USA.

<sup>5</sup>Now at Royal Netherlands Institute for Sea Research, Den Burg, Netherlands.

<sup>6</sup>School of Environmental Sciences, University of East Anglia, Norwich, UK.

<sup>7</sup>Biology Department, Woods Hole Oceanographic Institution, Woods Hole, Massachusetts, USA.

[3] The flux,  $F$ , of a sparingly soluble gas can be parameterized as the product of its air-water concentration difference and the gas transfer velocity, which embodies the details of the turbulence-mediated gas transfer across the surface aqueous mass boundary layer (SAMBL). Thus,

$$F = k(C_w - sC_a) \quad (1)$$

where  $s$  is the solubility coefficient,  $k$  is the gas transfer velocity, and  $C_w$  and  $C_a$  are the gas concentrations in the water and the atmosphere, respectively. Since field measurements of the concentration difference are usually straightforward to obtain in almost any type of aqueous system, the major challenge for modeling accurate fluxes has been to develop a quantitative model of  $k$ , which is influenced by turbulent mixing at the SAMBL due to a multitude of processes. The purpose of this report is to present field experimental evidence that a mechanistic model based on turbulence accurately predicts  $k$  for a wide range of processes that occur in a variety of environmental systems.

[4] Wind forcing has long been known to exert a major control on gas transfer as well as on near-surface turbulence, and many wind-forced processes have been suggested as mechanisms for the enhancement of both. Small-scale waves have been suggested as a dominant mechanism for  $k$  [Bock *et al.*, 1999] since wave slope is strongly linked with gas transfer. Microbreaking, or the breakdown of small-scale waves that do not entrain air, may explain the link between  $k$  and surface roughness and has been shown to directly enhance gas transfer at low to moderate wind speeds [Zappa *et al.*, 2001; Zappa *et al.*, 2004]. In the presence of surface films, near-surface turbulence is suppressed and  $k$  may be significantly reduced at a given wind speed or wind stress [Jähne *et al.*, 1987]. Surface contamination by thin organic films measured in the field has also been shown to dampen high frequency waves and leads to reduced gas exchange [Frew *et al.*, 2004]. Less dependence of  $k$  is observed on wind speed under conditions when buoyancy may dominate the production of turbulence in the near-surface layer [McGillis *et al.*, 2004] or when rain directly effects the turbulence at the interface and causes variability in  $k$  [Ho *et al.*, 2004]. In coastal systems, bottom-generated turbulence that is transported to the surface [Nimmo-Smith *et al.*, 1999] can significantly affect gas transfer and may represent a case in which both wind forcing and tidal currents generate turbulent energy [Borges *et al.*, 2004].

### 2. Conceptual Model

[5] Gas exchange continues to be very difficult to measure directly in the field, forcing researchers to use models

of  $k$ , and thereby the flux using equation (1) with concentration differences. Wind speed parameterizations [e.g., *Wanninkhof*, 1992] have long been used to estimate  $k$  in the open ocean, yet many of the processes that affect  $k$  are not directly related to wind forcing (e.g., tidal currents, rain, surfactants, wave fetch) in addition to more complicated interactions that preclude the use of this simplistic approach. Since turbulence in the aqueous boundary layer is known to drive the exchange of gases across the air-water interface and individual processes regulate the turbulence, many mechanistic approaches have also been suggested that include surface renewal [*Komori et al.*, 1993], surface penetration [*Atmane et al.*, 2004], and surface divergence [*McKenna and McGillis*, 2004; *Turney et al.*, 2005]. All these mechanistic approaches attempt to embody the turbulence that is driving the exchange but have shown limited applicability across a range of environmental conditions. In this report, the turbulent kinetic energy (TKE) dissipation rate,  $\varepsilon$ , is demonstrated to provide a measure to scale  $k$  based on the processes that directly control gas transfer across the air-water interface.

[6] The primary driving mechanism that regulates  $k$  across the air-water interface is presumed to be near-surface turbulence from low to moderate wind speeds (nominally below  $10 \text{ m s}^{-1}$ ). At higher winds, bubble-mediated exchange produced by breaking waves may play a significant role. The magnitude of  $k$  is determined by the temporal and spatial variation of the SAMBL and the molecular diffusivity of the gas in question. The thickness of this SAMBL is a function of near-surface turbulence. The turbulent transport can be explicitly related to the dissipation rate, a parameter that can be measured in the field. The resulting scaling relationship for gas transfer can be derived for diffusion across the SAMBL using the *Batchelor* [1959] scale  $\delta_B = Sc^{-1/2}\eta$ , where  $\eta = (\nu^3/\varepsilon)^{1/4}$  is the Kolmogorov, or dissipative, microscale [*Melville*, 1996] and the Schmidt number,  $Sc$ , is defined as the ratio of the kinematic viscosity of water,  $\nu$ , to mass diffusivity  $D$  of water. *Kitaigorodskii* [1984] derived an expression for  $k$  and the turbulent dissipation rate in the context of modeling the influence of patches of enhanced turbulence by breaking. *Lamont and Scott* [1970] derived a similar expression using surface renewal theory [*Danckwerts*, 1951] and *Banerjee et al.* [1968] for wavy turbulent liquid films. More recently, *Lorke and Peeters* [2006] have suggested a unified relationship for boundary layer transport based on  $\varepsilon$  for interfacial fluxes at both the benthic and air-sea boundary layers.

[7] Despite these different approaches, the dependence of gas transfer on turbulent transport and diffusivity can be modeled in the same form of:

$$k \propto (\varepsilon\nu)^{1/4} Sc^{-n}. \quad (2)$$

For the scaling in equation (2) to be rigorous, the value for  $\varepsilon$  is required to be that at the surface since the dissipation rate has various suggested dependencies with depth [*Anis and Moum*, 1995; *Terray et al.*, 1996]. The Schmidt number exponent  $n$  varies between  $2/3$  and  $1/2$  depending on the surface conditions. Surface contamination is known to modify the free-surface condition to behave as a rigid boundary by introducing a tangential stress that works to suppress horizontal motion, and therefore near-surface

turbulence. The conceptual model described by equation (2) demonstrates that increasing turbulence dissipation intensity will enhance  $k$ . Here we measure  $\varepsilon$  and  $k$  to test the scaling in equation (2) for the first time across several natural systems, processes, and forcings.

### 3. Methods

[8] Over the past 6 years we have conducted a series of studies using the gradient flux technique (GFT), the active controlled flux technique (ACFT), and measurements of  $\varepsilon$  in rivers, estuaries, and the coastal ocean. We have developed an easily deployed system for performing these measurements aboard the Surface Processes Instrument Platform (SPIP; see *Zappa et al.* [2003] for description), a small research catamaran that enables spatial sampling. We have utilized this setup in the Parker River Estuary, a small shallow macro-tidal estuary with limited fetch draining into the Gulf of Maine, and the tidal freshwater Hudson River in New York, USA. We have adapted this system for use in the model ocean of Biosphere 2 in Oracle, Arizona, USA [*Ho et al.*, 2004]. At the Field Research Facility (FRF) of the US Army Corps of Engineers in Duck, NC, USA, atmospheric scalar profiles were measured from a mast boomed out from the end of the pier and a subsurface mast system was deployed to measure dissipation beneath the waves.

[9] GFT measures the concentration gradient in the atmospheric surface boundary layer together with the eddy diffusivity based on Monin-Obhukov scaling to calculate the flux [*McGillis et al.*, 2001]. GFT was used to measure  $k$  for  $\text{CO}_2$  in the Parker and Hudson Rivers following *Zappa et al.* [2003], as well as for dimethyl sulfide (DMS) at the FRF in Duck, NC, USA. DMS fluxes were measured by the gradient flux method as in *Hintsa et al.* [2004], and  $k$  was calculated according to (1) using aqueous DMS concentrations. ACFT relies on heat as a proxy tracer for gas according to unsteady diffusion combined with surface renewal theory to estimate  $k$  [*Zappa et al.*, 2004]. ACFT was used to estimate  $k$  during the Parker River estuary studies as well as at Biosphere2 following *Zappa et al.* [2004; 2003]. An  $\text{SF}_6$  tracer addition was made to estimate  $k$  as in previous experiments at Biosphere 2 [*Ho et al.*, 2004]. All measurements of  $k$  have been scaled to a Schmidt number of 600.

[10] Estimates of  $\varepsilon$  were made using the inertial dissipation method following *Zappa et al.* [2003]. An acoustic Doppler velocimeter (ADV) sampled at 25 Hz was used in the Parker and Hudson Rivers at a nominal depth of  $O(10 \text{ cm})$ , as well as at the Field Research Facility at a nominal depth of  $O(1 \text{ m})$ . A pulse-to-pulse coherent Doppler profiler (DopBeam) directed vertically at the surface sampled at 375 Hz was used to provide near-surface fine-scale vertical profiles of  $\varepsilon$  at Biosphere 2 in addition to a Nobska modular acoustic velocity sensor (MAVS) at a depth of 50 cm. The vertical resolution of the ADV and DopBeam was roughly 1 cm. We have decided not to extrapolate the  $\varepsilon$  estimates at depth to the viscous sublayer due to the variety of processes and the breadth of potential models that could be implemented. This decision is supported by recent measurements of *Gemmrich and Farmer* [2004] who found that temporally averaged dissipation below the mean waterline remained

nearly constant. In the crest region, the dissipation increased up to a factor of only 1.6, which will result in a 10% effect on  $k$ .

#### 4. Results

[11] In March to April 2004, measurements of the turbulent dissipation rate and the flux of dimethyl sulfide (DMS) were made as a storm approached in the coastal ocean at the FRF. This coastal location provides the ability to isolate wind and waves, and we found that  $k$  and  $\varepsilon$  are related to both. Figure 1a shows wind speed, wave spectral density, dominant wave frequency, significant wave height, and turbulent dissipation rate. As the storm approached before Day 88, the dominant wave conditions consisted of old seas (wave age,  $C_p/U_{10} = 3$ , where  $C_p$  is the phase speed of the dominant wave and  $U_{10}$  is the wind speed measured at 10 m). During the storm event on Days 88–91, the wind speed increases, the dissipation rate increases, and the initially moderately narrow-banded wave field expands with strong high frequency wave activity as the storm develops. Here, the wind and pre-existing swell were aligned and the developing wave system is young ( $C_p/U_{10} = 0.5$ ). As the storm subsides, the wave field gradually diminishes while the dissipation abruptly decreases on Day 92.

[12] A second wind event occurs around Day 96, with comparable wind speeds though not as sustained and not aligned with the pre-existing swell. Here, the dissipation levels do not reach those from the earlier storm and neither do the waves. The waves increase slightly in total energy with a small shift to lower peak frequency. The storm and 2nd wind event provide a range of turbulent dissipation rates and gas exchange rates that are representative of the wind conditions that drive wave-related processes such as microbreaking and whitecapping. The measurements of  $\varepsilon$  are comparable to those in energetic mixed layers with values from  $10^{-6}$  to  $10^{-4}$   $\text{W kg}^{-1}$  [MacIntyre et al., 1995] and during conditions of breaking waves from  $10^{-5}$  to  $10^{-2}$   $\text{W kg}^{-1}$  [Agrawal et al., 1992; Terray et al., 1996]. While the relationship between the measurements of transfer velocity and wind speed shown in Figure 1b agrees qualitatively with the predictions using a quadratic [Wanninkhof, 1992] or a cubic [Wanninkhof and McGillis, 1999] parameterization, the variability in  $k$  is significant and not best described by wind speed.

[13] Estuaries and rivers not only experience wind, but also forcing from tidal currents. The Parker River macro-tidal estuary, located in northeastern Massachusetts, USA, has highly energetic tides making it an ideal place to investigate the interaction between wind and currents. Cumulative results from measurements made during very low wind periods ( $< 2$   $\text{m s}^{-1}$ ) in the Parker River in August 2000 (mean depth = 3.2 m; wind and tides aligned) demonstrated the effects of changes in tidal velocity alone on  $k$  [Zappa et al., 2003]. Measurements showed that during times of very low wind, gas exchange is controlled by tidal-driven surface turbulence within the aqueous surface boundary layer in rivers and estuaries. This was the first example of a direct link between tides and gas exchange in a river system. The turbulence generated by tides during very low wind speeds not only controlled  $k$ , but also generated values for  $k$  that were comparable to those predicted by wind-speed relationships at moderate winds. Furthermore,  $k$  varied with  $\varepsilon$  and the surface renewal rate, indicating the viability of the

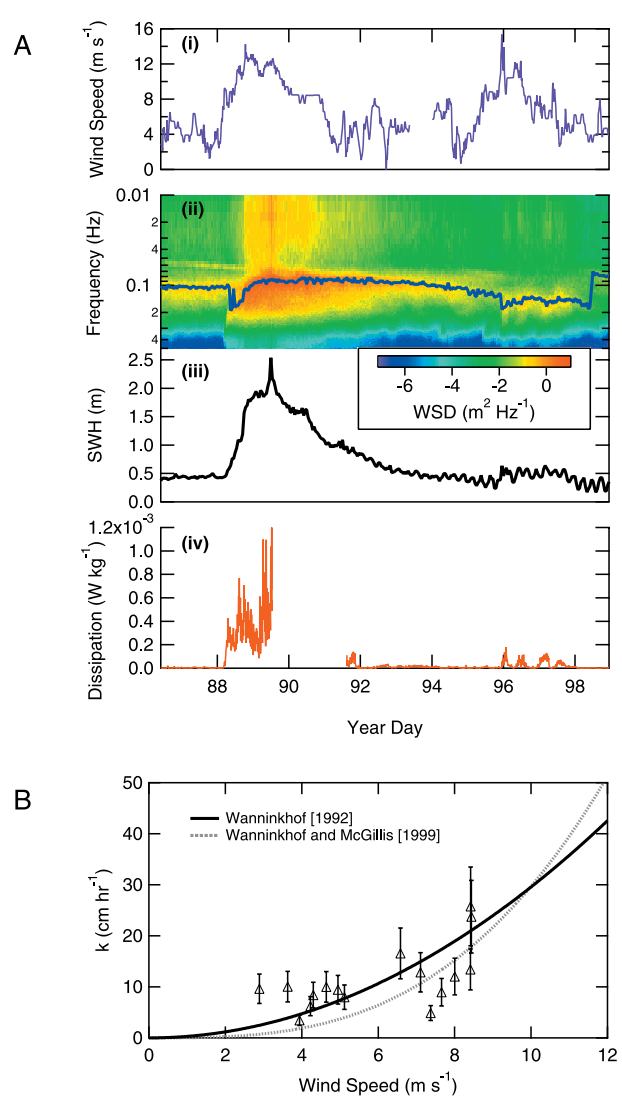


**Figure 1.** (a) Time series of wind speed (i), wave spectral density, WSD, i.e., the wave height variance per unit frequency (ii; color bar), dominant wave frequency (ii; blue trace), significant wave height, SWH (iii), and turbulent dissipation rate (iv). (b) Gas transfer velocity (triangles), determined by DMS gradients and scaled to a Schmidt number of 600, versus wind speed at 10 m. Data were taken during the Duck DMS Experiment at the Army Corps of Engineers Field Research Facility in Duck, N. C. in March to April 2004. Also plotted are quadratic [Wanninkhof, 1992] and cubic [Wanninkhof and McGillis, 1999] relationships for  $k$ .

surface turbulence index for embodying the processes affecting the gas transfer velocity. If the wind-speed relationships for estuaries [Raymond and Cole, 2001] were used under very low-wind conditions, estimates of  $k$  would have been less than 50% of those actually measured in the field.

[14] We have since measured  $k$  and  $\varepsilon$  at wind speeds up to  $10$   $\text{m s}^{-1}$  and recently have demonstrated important combined effects of wind and tides in this tidal-dominated system. Results from the Parker River in May 2002 (mean depth = 2.8 m; wind and tides aligned) in Figure 2a indicate

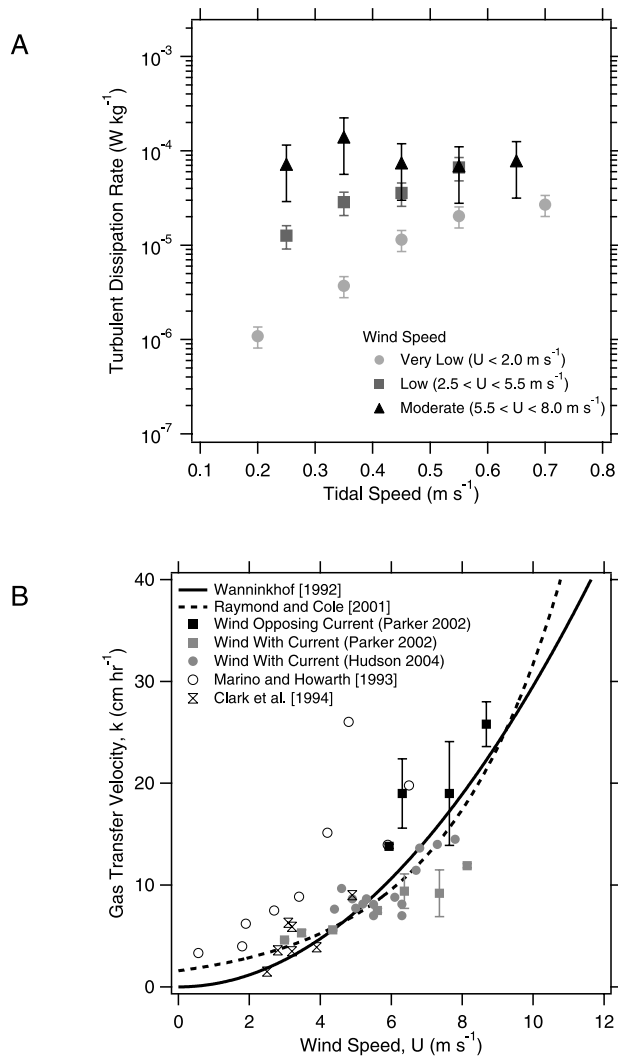


**Figure 2.** (a) Results show  $\varepsilon$  significantly varies with both wind speed and tidal speed. Measurements were made on the Parker River in May 2002 when the wind and current were aligned. (b) Gas transfer velocity versus wind speed in the Parker River Estuary and Hudson River. Transfer is enhanced when the wind and tidal currents oppose each other (black) compared to when the wind and tidal currents are aligned (gray). For comparison, floating dome [Marino and Howarth, 1993] and deliberate tracer [Clark et al., 1994] measurements from the Hudson River were added as well as the Wanninkhof [1992] relationship for  $k$  and the Raymond and Cole [2001] relationship determined from deliberate tracers in rivers and estuaries. A non-zero  $k$  at zero wind speed is consistent with the results of Zappa et al. [2003] and Borges et al. [2004] that showed that processes other than wind such as tidal currents influence  $k$ .

that our measurements of  $\varepsilon$  are able to resolve near-surface turbulence due to both wind and tides. As in Zappa et al. [2003], measurements of  $\varepsilon$  at low wind speeds show a strong correlation with tidal forcing. At moderately high wind speeds, however, the turbulent regime appears to have transitioned from tidal- to wind-driven turbulence since  $\varepsilon$  remains nearly constant as tidal speed increases. Furthermore, moderately high wind speeds did not ensure the

highest turbulent kinetic energy dissipation rates;  $\varepsilon$  could reach the levels produced by high winds when tidal velocities reached maximum values under low wind conditions. The Parker River data in Figure 2b also show that when winds are moving against the direction of tidal flow, the enhanced wind stress and the emergence of microbreaking enhances  $k$ . For the case of wind and current aligned, the wind stress is effectively less than it would be without the current and the value of  $k$  will be less. Alternatively, for the case of wind against the current, the wind stress is effectively greater than it would be without the current and the value of  $k$  will be greater as well because of the increased turbulent energy. According to Figure 2b, the interaction between opposing winds and tides may double  $k$  compared to when winds and tides are aligned.

[15] In shallow, macro-tidal systems such as the Parker River, the combined effect of wind and tides may create a scenario where  $k$  is higher than would be predicted using relationships from deeper, tidally-weak systems. We made measurements in a section of the tidal freshwater Hudson River in the summer of 2004 that was deeper ( $\sim 11$  meters), had a smaller tidal velocity range ( $2$  to  $44 \text{ cm s}^{-1}$ ), and had a longer average fetch ( $\sim 1 \text{ km}$ ) than the Parker River. Figure 2b shows a correlation between wind speed and  $k$  in the Hudson River when the wind and tidal current were aligned. Our data agreed well with a previous study on the Hudson River using a dual-tracer release [Clark et al., 1994], but provided values considerably lower than a previous study that used the floating dome technique [Marino and Howarth, 1993]. The interplay between wind and tides on the Hudson and Parker Rivers shows that considerable variability in  $k$  is not described well by published models for open-ocean or river and estuarine systems.

[16] Gas exchange can also be enhanced by raindrops that penetrate the water surface, generating a turbulent input of energy that is comparable to that of a moderate wind or current shear [Ho et al., 2004]. The model (i.e., artificial) saltwater ocean at Biosphere 2 (Oracle, AZ USA) provides an idealized system to investigate the effect of rain-induced turbulence on gas transfer. Measurements of turbulent dissipation rates using a pulse-to-pulse coherent Doppler profiler (DopBeam) directed vertically at the surface and of transfer velocity using the active controlled flux technique (ACFT) and  $\text{SF}_6$  tracer addition were made at Biosphere 2 in November 2003. The DopBeam data give profiles of dissipation rate near the air-water interface for the four rain events of similar strength in terms of rain rate. The profiles show an  $e^{-z}$  dependence, where  $z$  is depth positive downward, and average dissipation rates of  $1 \times 10^{-3} \text{ W kg}^{-1}$  at  $2 \text{ cm}$  below the surface and  $1 \times 10^{-4} \text{ W kg}^{-1}$  at  $15 \text{ cm}$  depth. This dependence is consistent with that suggested by Anis and Moum [1995] that high levels of turbulent kinetic energy at the surface, in this case generated directly by rain, are transported downward away from the surface by the motion of waves that are omnipresent in the model ocean. The background dissipation levels measured at roughly  $50\text{-cm}$  depth with the Modular Acoustic Velocity Sensor (MAVS) were  $5 \times 10^{-6}$  to  $8 \times 10^{-6} \text{ W kg}^{-1}$ . These background levels were significantly below those measured at the surface and indicative of the levels in the model ocean system before the rain event. Measurements of dissipation just below the

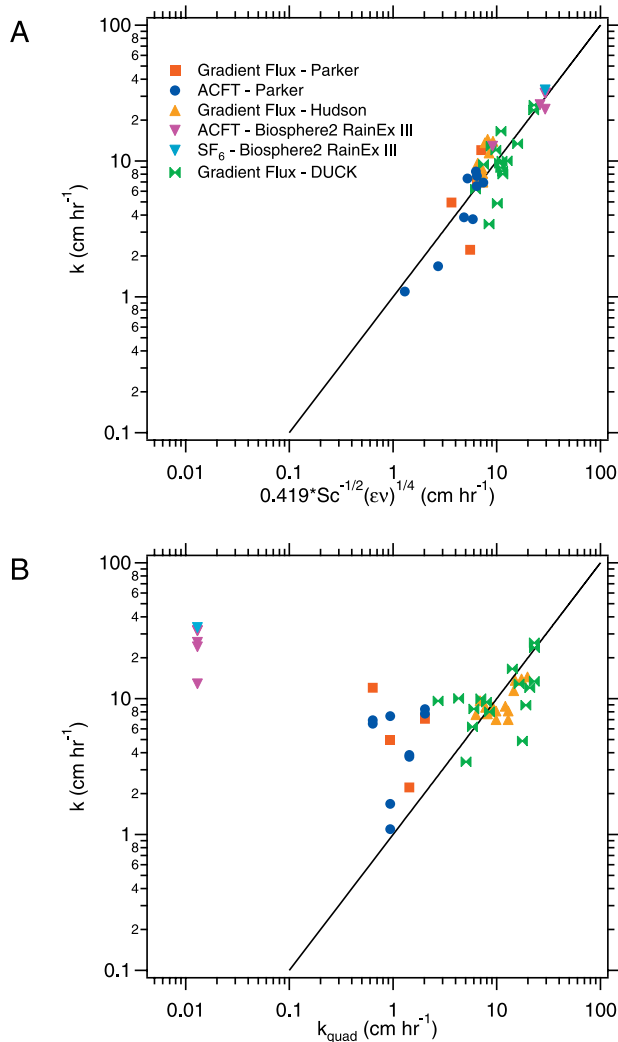


**Figure 3.** (a) Gas transfer velocity versus modeled  $k$  as determined from equation (2) in four separate systems that include the Parker River Estuary, the Hudson River, the coastal ocean off the FRF pier at Duck, N. C., and Biosphere 2 (rain, no wind or currents). (b) Gas transfer velocity versus modeled  $k_{quad}$  as determined from the Wanninkhof [1992] wind-speed parameterization for the same data as in Figure 3a. For those cases where there was no wind forcing (e.g., rain), a wind speed value of  $0.2 \text{ m s}^{-1}$  was used which is the lower bound implemented in the TOGA-COARE model to account for gustiness.

surface are more than an order of magnitude higher than those a few tens of cm's below. Magnitudes of  $\varepsilon$  at Biosphere 2 remained roughly constant from experiments in 2001 and 2003 considering that the measurement of  $\varepsilon$  at 20-cm depth from the DopBeam is nearly identical to that found using a single point acoustic Doppler velocimeter (ADV) sampling at 20-cm depth in the same model ocean under similar conditions [Ho et al., 2004].

## 5. Discussion

[17] Synthesizing all of these individual case studies indicates that dissipation rate controls gas exchange across

a variety of systems and environmental forcings as hypothesized. According to equation (2),  $k$  should scale with  $\varepsilon^{1/4}$ . Figure 3a shows  $k$  measured in a variety of vastly different systems that include the Parker River Estuary; the Hudson River; the coastal ocean at Duck, NC, and Biosphere 2 (rain; no wind) to be proportional to the model expressed in equation (2) with  $n = 1/2$ . The results clearly show that gas transfer scales with  $\varepsilon^{1/4}$  over a wide range of environmental systems with different types of forcing (i.e., wind, tides, rain). The constant of proportionality associated with equation (2) and used in Figure 3a was determined to be  $0.419 \pm 0.130$  by minimizing the root mean square difference ( $\pm 2.84 \text{ cm hr}^{-1}$ ) between the measured transfer velocities and the right-hand-side of equation (2). This constant of proportionality for equation (2) is nearly identical to the theoretical value of 0.4 [Lamont and Scott, 1970] calculated from first principles while roughly double that of previous experimental estimates from channel flows [Moog and Jirka, 1999] calculated empirically using the friction velocity based on the hydrostatic flow conditions and not using  $\varepsilon$  based on direct turbulence measurements. Figure 3b shows the same measured  $k$  as in Figure 3a versus transfer velocity,  $k_{quad}$ , estimated from the Wanninkhof [1992] quadratic wind speed parameterization. The root mean square difference is  $\pm 10.63 \text{ cm hr}^{-1}$  and significantly larger than for the dissipation rate scaling in Figure 3a. It is clear that the  $\varepsilon^{1/4}$  scaling shows a higher correlation than the Wanninkhof [1992] relationship (coefficient of determination of 0.93 versus 0.07), especially for the cases where processes other than wind (i.e., tidal currents and rain) drive the near surface turbulence that dominates the transfer.

[18] While the correlation in Figure 3a is robust,  $\varepsilon$  was measured at variable depths throughout these studies. An underlying assumption in equation (2) is that  $\varepsilon$  is measured directly at the water surface. Since the profile of turbulence near the air-water interface may be complicated by the interplay between wind, waves, current shear and other processes, measurements at depth will not be representative of  $\varepsilon$  at the surface because the profile changes nonlinearly with environmental forcing. For example, profiles of  $\varepsilon$  were measured during our rain experiments at Biosphere 2. The uppermost dissipation measurements at Biosphere 2 were made within a few cm of the surface using a DopBeam (versus 10–20 cm for the Parker and Hudson; 1–3 m for the coastal ocean at Duck, NC). The comparison of measured and modeled  $k$  using (2) for the Biosphere 2 data show less variability in Figure 3a even in the presence of significant salinity stratification developed from freshwater rain on the saltwater ocean. Thus, some of the scatter in Figure 3a may be due to the variable depths used in these studies. Profiles of  $\varepsilon$  are therefore required to improve our estimates of  $\varepsilon$  at the surface and gain a further understanding of the interplay between wind and currents and the transition between various forcing regimes.

## 6. Conclusion

[19] The results of the field studies demonstrate the feasibility of the proposed model for predicting  $k$  using the turbulent dissipation rate in a variety of environmental conditions, natural systems, and forcing mechanisms. Our results show that a universal scaling for gas exchange exists

based on the turbulent dissipation rate in the aqueous near-surface boundary layer. Based on these studies, we argue that more research is needed to gauge the effects of wind, tides, fetch, stratification, waves, and other processes on gas exchange from the open ocean to rivers and estuaries. Moreover, research is needed to relate  $\varepsilon$  to relevant, more easily measured, and even remotely-sensed, quantities. This would meet the growing need among scientists to elucidate and develop better models that reduce the uncertainty in predicting  $k$  when calculating the exchange rates of  $\text{CO}_2$  and other trace gases, performing nutrient studies, or determining volatile pollutant transport. As these new capabilities become more widely accepted and implemented, it would allow scientists to evaluate how spatial and temporal variation in  $k$  affects our ability to calculate the relative importance of  $\text{CO}_2$  fluxes in regional and global biogeochemical cycles.

[20] **Acknowledgments.** The authors wish to thank the staffs at the ACE-FRF, the PIE-LTER site, and Biosphere 2. This research was performed and the manuscript prepared with support from: the National Science Foundation (OCE-03-27256, OCE-05-26677, ATM 01-20569, and DEB-05-32075), the Office of Naval Research Young Investigator Program (N00014-04-1-0621), the Hudson River Foundation (010/02A), NOAA (NA03OAR4320179), the Marie Curie Training Site Fellowship (HPMF-CT-2002-01865), the NERC (NER/B/S/2003/00844), the David and Lucille Packard Foundation, and the LDEO Climate Center. This is LDEO contribution 7019.

## References

- Agrawal, Y. C., et al. (1992), Enhanced dissipation of kinetic energy beneath surface waves, *Nature*, *359*, 219–220.
- Anis, A., and J. N. Moum (1995), Surface wave-turbulence interactions: Scaling  $\varepsilon(z)$  near the sea surface, *J. Phys. Oceanogr.*, *25*, 2025–2045.
- Atmane, M. A., W. E. Asher, and A. T. Jessup (2004), On the use of the active infrared technique to infer heat and gas transfer velocities at the air-water free surface, *J. Geophys. Res.*, *109*, C08S14, doi:10.1029/2003JC001805.
- Banerjee, S., et al. (1968), Mass transfer to falling wavy liquid films in turbulent flow, *Ind. Eng. Chem. Fundam.*, *7*(1), 22–27.
- Batchelor, G. K. (1959), Small-scale variation of convected quantities like temperature in turbulent fluid. Part 1: General discussion and the case of small conductivity, *J. Fluid Mech.*, *5*, 113–133.
- Bock, E. J., et al. (1999), Relationship between air-sea gas transfer and short wind waves, *J. Geophys. Res.*, *104*, 25,821–25,831.
- Borges, A. V., et al. (2004), Gas transfer velocities of  $\text{CO}_2$  in three European estuaries (Randers Fjord, Scheldt, and Thames), *Limnol. Oceanogr.*, *49*(5), 1630–1641.
- Borges, A. V., B. Delille, and M. Frankignoulle (2005), Budgeting sinks and sources of  $\text{CO}_2$  in the coastal ocean: Diversity of ecosystems counts, *Geophys. Res. Lett.*, *32*, L14601, doi:10.1029/2005GL023053.
- Clark, J. F., et al. (1994), Gas exchange rates in the tidal Hudson River using a dual tracer technique, *Tellus, Ser. B.*, *46*, 274–285.
- Cole, J. J., and N. F. Caraco (2001), Carbon in catchments: Connecting terrestrial carbon losses with aquatic metabolism, *Mar. Freshwater Res.*, *52*, 101–110.
- Danckwerts, P. V. (1951), Significance of liquid-film coefficients in gas absorption, *Ind. Eng. Chem.*, *43*(6), 1460–1467.
- Feely, R. A., et al. (2001), The uptake and storage of carbon dioxide in the ocean: The global  $\text{CO}_2$  survey, *Oceanography*, *14*(4), 18–32.
- Frankignoulle, M., et al. (1998), Carbon dioxide emission from European estuaries, *Science*, *282*, 434–436.
- Frew, N. M., et al. (2004), Air-sea gas transfer: Its dependence on wind stress, small-scale roughness, and surface films, *J. Geophys. Res.*, *109*, C08S17, doi:10.1029/2003JC002131.
- Gemmrich, J. R., and D. M. Farmer (2004), Near-surface turbulence in the presence of breaking waves, *J. Phys. Oceanogr.*, *34*, 1067–1086.
- Hintsa, E. J., J. W. H. Dacey, W. R. McGillis, J. B. Edson, C. J. Zappa, and H. J. Zemmelenk (2004), Sea-to-air fluxes from measurements of the atmospheric gradient of dimethylsulfide and comparison with simultaneous relaxed eddy accumulation measurements, *J. Geophys. Res.*, *109*, C01026, doi:10.1029/2002JC001617.
- Ho, D. T., C. J. Zappa, W. R. McGillis, L. F. Bliven, B. Ward, J. W. H. Dacey, P. Schlosser, and M. B. Hendricks (2004), Influence of rain on air-sea gas exchange: Lessons from a model ocean, *J. Geophys. Res.*, *109*, C08S18, doi:10.1029/2003JC001806.
- Ho, D. T., C. S. Law, M. J. Smith, P. Schlosser, M. Harvey, and P. Hill (2006), Measurements of air-sea gas exchange at high wind speeds in the Southern Ocean: Implications for global parameterizations, *Geophys. Res. Lett.*, *33*, L16611, doi:10.1029/2006GL026817.
- Jähne, B., et al. (1987), On the parameters influencing air-water gas exchange, *J. Geophys. Res.*, *92*, 1937–1949.
- Kitaigorodskii, S. A. (1984), On the fluid dynamical theory of turbulent gas transfer across an air-sea interface in the presence of breaking wind-waves, *J. Phys. Oceanogr.*, *14*, 960–972.
- Komori, S., et al. (1993), Turbulence structure and mass transfer across a sheared air-water interface in wind-driven turbulence, *J. Fluid Mech.*, *249*, 161–183.
- Lamont, J. C., and D. S. Scott (1970), An eddy cell model of mass transfer into the surface of a turbulent liquid, *AIChE J.*, *16*, 512–519.
- Lorke, A., and F. Peeters (2006), Toward a unified scaling relation for interfacial fluxes, *J. Phys. Oceanogr.*, *36*, 955–961.
- MacIntyre, S., et al. (1995) Trace gas exchange across the air-water interface in freshwater and coastal marine environments, in *Biogenic Trace Gases: Measuring Emissions from Soil and Water*, edited by P. A. Matson and R. C. Harriss, pp. 52–97, Blackwell Sci., Cambridge, Mass.
- Marino, R., and R. W. Howarth (1993), Atmospheric oxygen exchange in the Hudson River: Dome measurements and comparison with other natural waters, *Estuaries*, *16*(3a), 433–445.
- McGillis, W. R., et al. (2001), Carbon dioxide flux techniques performed during GasEx-98, *Mar. Chem.*, *75*, 267–280.
- McGillis, W. R., et al. (2004), Air-sea  $\text{CO}_2$  exchange in the equatorial Pacific, *J. Geophys. Res.*, *109*, C08S02, doi:10.1029/2003JC002256.
- McKenna, S. P., and W. R. McGillis (2004), The role of free-surface turbulence and surfactants in air-water gas transfer, *Int. J. Heat Mass Transfer*, *47*, 539–553.
- Melville, W. K. (1996), The role of surface-wave breaking in air-sea interaction, *Annu. Rev. Fluid Mech.*, *28*, 279–321.
- Moog, D. B., and G. H. Jirka (1999), Air-water gas transfer in uniform channel flow, *J. Hydraul. Eng.*, *125*(1), 3–10.
- Nimmo-Smith, W. A. M., et al. (1999), Surface effects of bottom-generated turbulence in a shallow tidal sea, *Nature*, *400*, 251–254.
- Raymond, P. A., and J. J. Cole (2001), Gas exchange in rivers and estuaries: Choosing a gas transfer velocity, *Estuaries*, *24*(2), 312–317.
- Richey, J. E., et al. (2002), Outgassing from Amazonian rivers and wetlands as a large tropical source of atmospheric  $\text{CO}_2$ , *Nature*, *416*, 617–620.
- Sweeney, C., M. M. Gloor, A. R. Jacobson, R. M. Key, G. McKinley, and J. L. Sarmiento (2007), Constraining global air-sea gas exchange for  $\text{CO}_2$  with recent bomb  $^{14}\text{C}$  measurements, *Global Biogeochem. Cycles*, doi:10.1029/2006GB002784, in press.
- Takahashi, T., et al. (2002), Biological and temperature effects on seasonal changes of  $\text{pCO}_2$  in global surface ocean, *Deep Sea Res., Part II*, *49*, 1601–1622.
- Terray, E. A., et al. (1996), Estimates of kinetic energy dissipation under surface waves, *J. Phys. Oceanogr.*, *26*, 792–807.
- Turney, D. E., W. C. Smith, and S. Banerjee (2005), A measure of near-surface fluid motions that predicts air-water gas transfer in a wide range of conditions, *Geophys. Res. Lett.*, *32*, L04607, doi:10.1029/2004GL021671.
- Wanninkhof, R. (1992), Relationship between wind speed and gas exchange over the ocean, *J. Geophys. Res.*, *97*, 7373–7382.
- Wanninkhof, R., and W. R. McGillis (1999), A cubic relationship between air-sea  $\text{CO}_2$  exchange and wind speed, *Geophys. Res. Lett.*, *26*, 1889–1892.
- Zappa, C. J., et al. (2001), Microscale wave breaking and air-water gas transfer, *J. Geophys. Res.*, *106*, 9385–9391.
- Zappa, C. J., et al. (2003), Variation in surface turbulence and the gas transfer velocity over a tidal cycle in a macro-tidal estuary, *Estuaries*, *26*(6), 1401–1415.
- Zappa, C. J., W. E. Asher, A. T. Jessup, J. Klinke, and S. R. Long (2004), Microbreaking and the enhancement of air-water transfer velocity, *J. Geophys. Res.*, *109*, C08S16, doi:10.1029/2003JC001897.

J. W. H. Dacey, Biology Department, Woods Hole Oceanographic Institution, Woods Hole, MA 02543, USA.

J. B. Edson, Department of Marine Sciences, University of Connecticut, Avery Point, Groton, CT 06340, USA.

D. T. Ho, W. R. McGillis, and C. J. Zappa, Lamont-Doherty Earth Observatory, Columbia University, Palisades, NY 10964, USA. (zappa@ldeo.columbia.edu)

P. A. Raymond, School of Forestry and Environmental Studies, Yale University, New Haven, CT 06511, USA.

E. J. Hintsa, Department of Chemistry and Chemical Biology, Harvard University, Cambridge, MA 02138, USA.

H. J. Zemmelenk, Royal Netherlands Institute for Sea Research, P.O. Box 59, NL-1790 AB Den Burg, Netherlands.